Catalysis Science & Technology

Accepted Manuscript

ROYAL SOCIETY OF CHEMISTRY

www.rsc.org/catalysis

Selective Hydrodeoxygenation of Bio-Oil Derived Products: Ketones to Olefins

Ayut Witsuthammakul[a] and Tawan Sooknoi[a,b]*

Abstract

The hydrodeoxygenation (HDO) of various ketones (acetone, methyl ethyl ketone and cyclohexanone) to olefins via hydrogenation - dehydration was conducted in fixed bed reactor at 373 – 573 K under H_2. Ketone can be hydrogenated over the metal function to alcohol intermediate that is subsequently dehydrated to olefin over the acidic function. A preliminary study on hydrogenation of acetone to 2-propanol over metal/SiO_2 catalysts (Cr, Fe, Co, Ni, Cu and Pd) shows that Ni and Cu are active at > 373 K. Although Ni possesses an activity higher than that of Cu, it promotes olefin hydrogenation and alcohol hydrogenolysis at > 473 K. Hydrogenolysis of the alcohol intermediates can be reduced over Ni-Cu alloy. An optimum conversion with 100% selectivity to alcohol, can be obtained at 448 and 473 K for Ni and Cu, respectively. The dehydration of 2-propanol to propylene over proton zeolites (ZSM-5, Y, Mordenite and β) can be achieved at > 398 K. The zeolites with three-dimensional pore structure (β and Y) provide relative higher activity (> 90% conversion). However, a bimolecular dehydration to ether is also promoted. Only HZSM-5 shows excellence selectivity to propylene (98 %). Hydrodeoxygenation of ketones was tested with

(i) Double bed of 5%Ni/SiO_2 and HZSM-5 (Si/Al~13), (ii) physical mixed bed of 5%Cu/SiO_2 and HZSM-5 (Si/Al ~13) and (iii) bi-functional catalyst of 5% Cu/HZSM-5 (Si/Al ~250). It was found that high alkene selectivity was readily obtained at 448 K. While, over the physical mixed bed and bi-functional catalyst, the hydrogenation activity was enhanced as the alcohol intermediate was removed from the system. The reactivity of ketone depends on their adsorption on the metal surface and steric hindrance, i.e. acetone > cyclohexanone > methyl ethyl ketone.

1. Introduction

Nowadays, the application of pyrolysis bio-oil is limited because approximately 20-50 % oxygen is retained in the products.[1-3] Therefore, the upgrading of pyrolysis bio-oil is necessary. Many researchers suggest that almost all oxygen can be removed by hydrotreatment process. However, a large amount of hydrogen is consumed and the saturated oxygen-free compounds[4-7] cannot be used as chemical feedstock. Accordingly, mild hydrodeoxygenation is of interest to remove oxygen functional groups and produce olefins as reactive hydrocarbon feedstock. For example, mild hydrodeoxygenation of acetone can produce propylene that can be used to produce valuable C3 chemicals e.g. acrylic acid and acrylates,[8-10] acrylonitrile,[11-12] pyridine[13] propylene oxide and 1,2-propane-diol,[14-16] and the most consumed polymer, polypropylene.[17-18]

Aliphatic and cyclic ketones are common oxygenate compounds found in bio-oil[19-23] and a lot more in the upgrading of bio-oil via ketonization process.[24-26] The decarbonylation as done for aldehydes is impossible for the ketones. The direct reduction usually leads to formation of paraffin or alcohol when drastic or mild condition is used, respectively.[27-30] It seems that multi-step reaction on one or more catalyst system is required. A similar idea to produce acrylic acid from glycerol via an integration of dehydration-oxidation[31] can be applied for mild hydrodeoxygenation of ketones to olefins. In this case, the ketone can be primarily hydrogenated to alcohol that is subsequently dehydrated to olefin. However, the nature of sub-reactions is different. For example, hydrogenation is preferred at relatively low

temperature and high pressure while dehydration is promoted at higher temperature and lower pressure. In the catalytic point of view, the acid function should promote only dehydration of the alcohol product, but not aldol condensation of the ketone fed. In the same view, the metal function should be selective only for hydrogenation of the ketone to alcohol, not the olefin to paraffin. Accordingly, several parameters have to be adjusted and controlled including competitive adsorption of feed, intermediates and products on each individual active site.

In this work, a catalytic system designed for mild hydrodeoxygenation of ketone to olefin was investigated. Hydrogenation of ketone to alcohol was accomplished over metal catalysts (Ni, Cu, Fe, Co, Pt and their alloys) at low temperature.[32-35] The alcohol produced was then dehydrated over acidic catalysts (γ-Al_2O_3, HZSM-5, HY and H-Beta).[36-39] Hydrogenation and dehydration were separately studied in order to understand the role of each catalytic function. The integrated hydrogenation-dehydration over double bed, physical mixed bed and bi-functional catalyst bed were then optimized to allow only essential amount of hydrogen consumption in the first stage. The olefins were selectively obtained and the reactivity of different ketones were compared and discussed.

2. Experimental procedure

As zeolites with various Si/Al are used in this study, the Si/Al of a particular sample is designated as a number in the parenthesis; i.e. a HZSM-5 sample with Si/Al~13 is referred to as HZSM-5 (13). HZSM-5 (13) and HZSM-5 (250) were obtained from Zeochem® and HZSM-5 (180) were obtained from Zeolyst®. NH_4^+-Beta (14), H-Mordenite (15), NH_4^+Y (3.5) and HY (100) were supplied by Tohso. The NH_4^+-zeolites were converted to H^+-zeolites by calcination at 773 K under flow of air zero (60 mL/min) for 5 h with a heating rate of 2 K/min. Metal supported catalysts were simply prepared by incipient wetness impregnation. Metal nitrate precursors ($Cu(NO_3)_2.3H_2O$ by Ajax Fine Chem, $Ni(NO_3)_2.6H_2O$, $Cr(NO_3)_3.9H_2O$ $Fe(NO_3)_3.9H_2O$, and $Co(NO_3)_2.6H_2O$ by Carlo Erba®) were dissolved in deionized water (~0.01 M) and slowly drop onto support (SiO_2; Carlo Erba and Zeolites) until wet. The sample was dried at 333 K in an oven for 15 min, and then the loading was repeated until desired metal content was reached. The samples were kept to dry at 333 K overnight and calcined in air zero (60 $ml.min^{-1}$) at 723 K for 5 h, then pelletized to the size of 600–850 μm.

Elemental composition was determined by X-ray fluorescence spectrometer (XRF; Siemens). Specific surface area (BET) of catalysts was measured using nitrogen adsorption analyzer (Quantachrome) at 77 K and 0.05–0.30 P/P_0. Residue retained in the used catalysts was analysed by thermo-gravimetric analysis (Perkin Elmer) under air-zero or N_2 stream from 323 - 1173 K at rate of 10 K/min. Reducible metal oxide species in the catalysts was

analyzed by temperature programmed reduction (TPR). The catalysts were treated in air-zero at 723 K for 5 hours prior to heating from 323 - 1173 K in 10% H_2/Ar. The hydrogen consumption was recorded with an on-line thermal conductivity detector (VICI).[40-41] Copper dispersion on support was also analyzed by selective surface TPR technique. Briefly after typical TPR, the sample was *in situ* treated with N_2O at 333 K for 2 hours. Then, the surface-oxidized sample was subjected to a secondary TPR.[42] Moles of surface copper can be calculated as described by Sagar *et al.*[43] Acidity of HY and Cu/HY was quantified by NH_3-TPD. 1 % NH_3/He was pre-adsorbed at 323 K. TPD was carried out in He at 10 $K.min^{-1}$ from 323 – 973 K.[44]

The catalytic testing was conducted in a fixed bed flow reactor (6 mm i.d. Pyrex®). The catalysts were primarily activated at 723 K (2 $K.min^{-1}$) under stream of air zero (30 $ml.min^{-1}$) for 5 h. Subsequently the metal supported catalysts were treated in H_2 at 723 K for 2 h. The system was cooled down to the reaction temperature (373 – 573 K) and the ketone feed was introduced by a syringe pump at a rate of 0.07-0.7 $g.h^{-1}$. The reaction was carried out for 9 h on stream and the products were analyzed by an on-line GC-FID every 70 minutes. A Hayesep® P (1/8" X 8') was used as separating column.

3. Result and discussion

3.1 Catalyst characterization

Metal content and surface area of all catalyst samples are tabulated in Table S1 (supplementary information). All catalysts possess relatively high surface area. The copper dispersion on SiO_2 decrease from 95 to 24 % when loading was increased from 5 - 15% (Table 1). However, the dispersion for 2% Cu/SiO_2 cannot be accurately calculated, presumably due to an incomplete surface oxidation by N_2O and a deviated hydrogen consumption measurement when the Cu loading is relatively small. The relatively lower Cu dispersion is observed when zeolites are used as support (54 – 65 %). This is possibly because, with this technique, part of the surface Cu oxide may well become exchangeable Cu cation that cannot be easily reduced. The presence of exchangeable copper cation in HY can be evidenced from an obvious increase in weak acidity, as compared to that in the parent HY (Table 1).

Figure 1 shows that at 2 wt% loading on silica, high temperature is required for reduction of Cr >Co~Fe >Ni >Cu oxides, respectively.[45] Broad reduction peaks at the shoulder of CuO and NiO at 650-800 K are attributed to various metal support interactions including copper or nickel silicate.[46-47] While, cobalt oxide reduction appears as two peaks at 548 and 643 K, corresponded to $Co_3O_4 \rightarrow CoO$ and $CoO \rightarrow Co$, respectively.[48-49] For iron oxide, the first reduction peak of iron corresponds to two overlap stage $Fe_2O_3 \rightarrow Fe_3O_4$ and

120 $Fe_3O_4 \rightarrow FeO$ (603 K).[50] While, fully reduction of FeO to Fe cannot be observed up to 1173
121 K. The formation of Fe_2SiO_4 is expected as a cause of incomplete reduction.[51] The TPR
122 profile of chromium oxide corresponds to the reduction of dichromate and poly chromate to
123 Cr_2O_3 (700 K).[52] However, chromium (III) is very stable and cannot be reduced in this
124 temperature range.[53] When nickel and copper are mixed on silica, the complete alloys are
125 obtained at every composition as seen by single hydrogen consumption peak in Figure S1
126 (supplementary information).

127 The copper loaded HY (100) and HZSM-5 (250) show two reduction peaks at 470 K,
128 corresponding to CuO aggregates on the surface (Figure 2). The higher temperature peak
129 (520 K) is defined as highly dispersed copper oxide in the pore of zeolites.[54-55] It is noted that
130 higher Cu dispersion is observed on HY, as compared to HZSM-5, presumably due to a better
131 diffusion of Cu precursor in the larger pore (peak at ~520 K).

132

3.2 Hydrogenation

Since the successive hydrogenation of olefin product is not preferred, different metal catalysts are tested for selective hydrogenation of ketone. As seen in Table 2, the initial activated temperature for hydrogenation of acetone and propylene for various metal catalysts are compared. The initial activated temperature reported in this study refers to the temperature at which >3% conversion is obtained over the catalyst at the same contact time (30 $g.h.mol^{-1}$). It is clear that chromium and iron are inactive for hydrogenations at low temperature. This is presumably due to an incomplete reduction of the metal phase under the condition investigated (723 K). However, 10%Fe/SiO_2 shows some activity for hydrogenation of acetone and propylene at temperature higher than 473 and 573, respectively. Co, Ni, Pd[56-57] catalysts are active for both acetone and propylene hydrogenation. Hydrogenolysis can also be promoted over these metals at relatively higher temperature. For acetone hydrogenation, the activity appears to be in the order of Ni > Pd >Co. In the opposite view, Pd is more active than Co and Ni for propylene hydrogenation. Copper seems to be the best choice for mild hydrogenation of acetone. Ketone can be hydrogenated (< 373 K) to alcohol without paraffin productions. The alloy with Ni (NiCu) significantly reduces both hydrogenation of propylene and hydrogenolysis acivity, as compared to the Ni alone. This is attributed an increase in oxophillicity of the surface when Cu is alloyed.[58] Hence, the interaction of C=C would be readily modified. In addition, the Cu alloying would strongly affect a structure sensitive reaction, such as hydrogenolysis. Both Ni

and Cu catalyst shows excellence catalyst stability and no carbon deposit can be observed by TGA of the spent catalysts (Table 3).

As Ni and Cu selectively promote hydrogenation of ketone with minimal activity for olefin hydrogenation, these catalysts are particularly studied for acetone hydrogenation at 373 - 573 K as shown in Figure 3. It can be seen that for both metals, acetone conversion increased with temperature until the thermodynamic limitation[59-61] is reached for the reaction conditions used in this study. The maximum conversion was obtained at 448 K for nickel and 473 K for copper. It is clear that the nickel is more active than the copper. 100% Selectivity to 2-propanol is obtained over the nickel catalyst at 373 - 448 K. However, hydrogenolysis to methane can be observed at > 473 K. Accordingly, the conversion obtained at this temperature is slightly higher than the equilibrium conversion of acetone to *2-p*roanol[61]. Meanwhile, C-O single bond breaking is unusual over copper; hence, excellent selectivity to 2-propanol was obtained over the copper at temperature up to 573 K. Figure S2 (supplementary information) emphasizes the thermodynamic limitation for acetone hydrogenation over copper catalyst. Although higher rate can be obtained at higher reaction temperature (473 K), the conversion levels at ~ 50%. At lower temperature (~ 448 K), the conversion can be boosted up at higher contact time. It is worth noting that 2-propanol is the only product over the copper catalyst despite the contact time has reached equilibrium. For further investigation, the contact time in this work was tested within 80 g.h.mol^{-1}.

Effect of nickel and copper loading on SiO_2 was studied (5-40 wt%) as shown in Figure 4. When the metal loading is increased, acetone conversion is enhanced due to an increase in number of active sites. The turnover frequency for all Cu/SiO_2 catalyst is roughly 2.1-2.8 x 10^{-3} sec^{-1}, as shown in Table S2 (supplementary information). However, the normalized rate (mole of feed converted per hour over mole of the metal loaded) is decreased due to agglomeration of the metal particles, which notably reduces the active metal surface (Table 1). In case of nickel catalyst, the increased metal particle size also leads to an increase hydrogenolysis activity, as seen from Figure 4a. The Ni catalysts with > 10% loading yield significant amount of methane (~30%). Meanwhile, copper retains its excellent selectivity towards C=O hydrogenation. This suggests that only η-1 adsorption mode is allowed for C=O on Cu surface.[58] Hence, 100% selectivity to 2-propanol is obtained over Cu catalyst up to 40% loading.

As methane was produced over the nickel catalyst at > 473 K, copper was mixed into the Ni catalyst to retard the methane formation. Theoretically, nickel and copper are miscible in wide range of component[62], as evidenced by TPR (Figure S1). It is clear from Figure 5 that the conversion is generally decreased with copper content in the alloy. A synergistic effect observed at ~ 25%Cu is presumably due to a better dispersion of the metal phase. At 473 K, no methane is observed from the catalysts with Cu content higher than 40 %. This is because of the hydrogenalysis is a structure sensitive reaction, alloying with Cu shall readily inhibits the adsorption mode that leads to C-C cleavage.[63]

192 **3.3 Dehydration of isopropanol**

193 Dehydration of the hydrogenated product, 2-propanol was separately investigated
194 over H-β catalyst at 448 K. Figure 6 shows that 2-propanol conversion increased with the
195 contact time. Two products, propylene and diisopropyl ether are initially observed in parallel
196 from an intra-molecular dehydration and inter-molecular dehydration, respectively. However,
197 the ether drops gradually at higher contact time (1.5-4.7 g.h.mol^{-1}). This indicates that the
198 ether can be converted to propylene and 2-propanol[64], as demonstrated by the reaction of
199 diisopropyl ether over H- β (Table 4) and below.

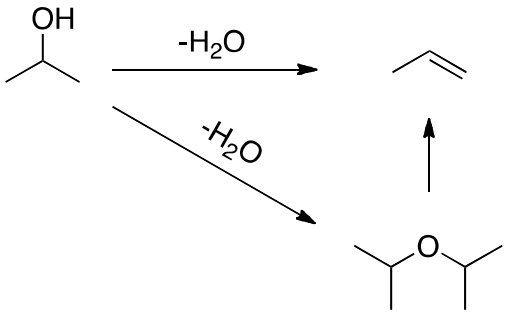

200

201 As also seen from Table 4, zeolite Y and β provide relatively higher activity, as
202 compared to other zeolites. However, the cage structure of Y can retain both feed and
203 products, which promotes the inter-molecular dehydration, as observed with high diisopropyl
204 ether selectivity at low contact time (3 g.h.mol^{-1}). In addition to the structural effect, a closer
205 site-proximity in HY (Si/Al ~8), as compared to that of H-β (Si/Al ~14) would enhance the
206 bimolecular dehydration. This also leads to a more rapid deactivation, as seen from a
207 relatively lower activity of HY after 6 h on stream, despite the acidity of HY is higher.

208 At higher contact time (15 g.h.mol^{-1}), it is clearly observed that the catalyst with three
209 dimensional pore opening (H-β) provides higher activity, as compared to those with two and
210 one dimensional pore opening (HZSM-5 and H-Mordenite), respectively. With a comparable
211 Si/Al, this suggests that diffusivity of the feed and products plays important role on
212 dehydration at relative low temperature (448 K). With poor mass transfer, re-hydration may
213 well take place at high contact time. Hence, mordenite gives even lower activity; as compared
214 to ZSM-5 despite the pore size is larger. In addition to the observed activity, ZSM-5 yields
215 only 2% di-isopropyl ether at 55 % conversion while β gives 10% di-isopropyl ether at
216 similar conversion. The result indicates that the medium pore size of ZSM-5 somewhat
217 constrains the size of intermediates and products while the large pores of β provides intrinsic
218 space for the bimolecular reaction. Moreover, the large one-dimensional pore system
219 particularly enhances the inter-molecular dehydration as the feed can be exceedingly retained
220 in the pore. In line with this view, thermogravimetric analysis shows that < 1 % hard coke is
221 detected on the used zeolite with medium pore while > 3 % is observed for the larger ones
222 (Table 3). The TGA under N_2 defines that most of deposits in HZSM-5 are the high
223 molecular weight compounds that cannot diffuse out of pore at the reaction temperature.

224 From Figure 7a, it can be seen that 2-propanol conversion is increased with the
225 temperature. Selectivity to propylene is also increased with the decrease in di-isopropyl
226 ether. This is simply because elimination of di-isopropyl ether to propylene is promoted at
227 high temperature. Again, the effect of pore size is revealed particularly at lower temperature.

228 When H-β was used (Figure 7b), similar pattern to H-ZSM-5 was observed. As discussed
229 earlier, β possesses higher activity, as compared to ZSM-5, but higher selectivity to di-
230 isopropyl ether at low temperature. No higher hydrocarbon was detected for both catalysts at
231 this temperature range, presumably due to the strong adsorption of the feed and ether over the
232 acid sites.

233

3.4 Ketones hydrodeoxygenation to olefins

In this work, hydrogenation – dehydration approach was employed for ketone hydrodeoxygenation. To combine the two reactions with exothermic and endothermic nature into one process, temperature has to be primarily optimized. For nickel - zeolite system, hydrogenation with no hydrogenolysis takes place at 373 - 448 K (Figure 3). While dehydration rate increases significantly above 423 K (Figure 7). Accordingly, only small gap from 423 to 448 K is allowed for a consecutive hydrogenation-dehydration over Ni/SiO_2-zeolite system, as illustrated below

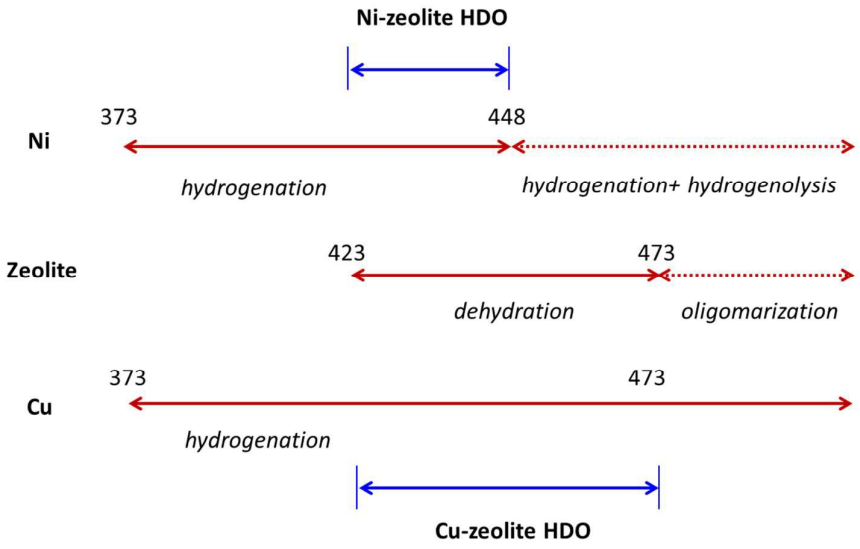

For Cu/SiO_2 - zeolite system, no hydrogenolysis can be promoted up to 575 K (Figure 3). However, the reaction over acid site is limited at 473 K to avoid the drastic oligomerization.[65] Accordingly, the window for hydrodeoxygenation over Cu/SiO_2 - zeolite system is widely opened (423 – 473 K), as illustrated above.

Therefore, the temperature at 448 K was selected for Ni/SiO_2 - zeolite system to obtain the maximum dehydration rate without hydrogenolysis. Since olefin hydrogenation can also be promoted over Ni/SiO_2 (Table 2), the hydrodeoxygenation is conducted in two-bed system. The ketone is hydrogenated over Ni/SiO_2 to an alcohol that becomes a feed for the dehydration to olefin over the zeolite bed. On the other hand, hydrogenation of olefin cannot be promoted over copper catalyst. Hence, single bi-functional bed system can be used for hydrodeoxygenation over Cu/SiO_2 - zeolite catalyst. A higher temperature (at 473 K) was chosen to obtain highest hydrogenation rate without oligomerization of the olefin products. However, an undesirable condensation of acetone may take place over the acid sites. Moreover, the ketone hydrogenation activity is relatively low, as compared to that of the alcohol dehydration, as observed from Figure 4 and Figure 6. Accordingly, the metal component in the bi-functional bed system has to be greater than that of the zeolite.

Double bed system of Ni/SiO_2 – zeolite

For this system, HZSM-5 was used to minimize the ether formation (Figure 7). Table 5 shows that up to 60 % conversion can be obtained at 76+7 $g.h.mol^{-1}$. However, 2-propanol and di-isopropyl ether, which are intermediates, still remain in large amount. By increasing the zeolite bed (76+27 $g.h.mol^{-1}$), only 10 % 2-propanol is observed without ether. The propylene is produced selectively (90% mol). No aldol product derived from the condensation of acetone on zeolite is detected. This is probably because of strong adsorption of alcohol that prevents the ketone condensation. However, a slight deactivation can be

observed for the dehydration bed. This is concluded from a gradual decline in propylene selectivity while the acetone conversion remains unchanged over 7 hours on stream (Figure 8). When a larger ketone, methyl ethyl ketone (MEK), is tested, a similar activity is obtained (~60 %). However, relative low selectivity to the alcohol (2-butanol) is observed due to the higher reactivity of butanol, as compared to propanol. Again, no ether and aldol product are detected for hydrodeoxygenation of MEK. This is presumably due to a larger steric constrain of any C4 species in the zeolite pore which inhibits the bi-molecular reaction (either etherification of the alcohol and aldol condensation of the ketone). Hence, the butanol produced from MEK hydrogenation is selectively dehydrated to *n*-butene (1-butene + 2-butene; 87%), and then isomerization to *i*-butene (13%).

Physical Cu/SiO_2 – zeolite mixed bed

For a single mixed bed, 5% Cu/SiO_2 was physically mixed with the zeolites using high metal/zeolite ratio at 473 K to prevent the condensation of ketone. From Table 6, it is seen that 68 % conversion with excellent selectivity to propylene (96 %) is obtained over the 76+7 bed (For contact time, 76+7 refers to 76 g.h.mol-1 of Cu/SiO2 and 7 g.h.mol-1 of HZSM-5; 83 g.h.mol-1 in total). A significant improvement in acetone conversion over the mixed bed, as compared to the equilibrium value (39% at 473 K, Figure 3) for acetone-alcohol, is presumably due to a simultaneous conversion of 2-propanol to propylene over the acid catalyst. This will noticeably reduce the rate of 2-propanol dehydrogenation to acetone, and hence draw the conversion of the acetone beyond such equilibrium level. With this

287 catalyst composition and reaction conditions, no condensation products from acetone is
288 observed. In fact, small amount 2-propanol (3 %) is intentionally retained to inhibit the
289 condensation of the ketone.

290 However, when H-β (14) is primarily mixed (76+7 g.h.mol^{-1}), deactivation is severe.
291 The acetone conversion at 6 hours on stream drops drastically, as compared to ZSM-5. This
292 is because β possesses a larger pore size, as compared to ZSM-5. This facilitates a better
293 diffusion and adsorprtion of acetone in the pore of β. Hence, relatively less fraction of the
294 acetone interact with the metal surface and hydrogenation is limited. In line with this view,
295 the aldol products namely mesityl oxide, acetic acid and *i*-butene (~ 20% in total) is instead
296 produced, as previously observed in literatures[66-67]. Since aldol condensation is largely
297 pronounced, high molecular weight deposits (Table 3) and a rapid deactivation can be
298 expected. Accordingly, reducing the contact time of β to 2 g.h.mol^{-1} can offer 92 % propylene
299 selectivity without the condensation products. However, the acetone conversion is still lower
300 than that over Cu/SiO_2/HZSM-5.

301 When larger ketone (i.e. MEK) is tested over 5% Cu/SiO_2 - HZSM-5 mixed catalyst
302 (Table 7), the conversion (56 %) is slightly lower than the acetone. This is probably due to
303 steric hindrance of the adsorbed ketone on the metal surface. High selectivity to 1-butene and
304 2-butene (82 %) was observed with some isomerization products (*i*-butene; 14 %) and 2-
305 butanol (4 %). For larger cyclic ketone, cyclohexanone is more reactive than the aliphatic
306 ketone. 96 % selectivity to cyclohexene is obtained with some methylcyclopentenes (4 %).

This is presumably due to the stronger adsorption of cyclohexanone, as compared to those of acetone and MEK. It is also worth noting that reducing the reaction temperature or contact time affects the dehydration rate significantly.

Bi-functional catalyst: Cu/zeolites

As high selectivity to olefin can be observed over Cu/SiO_2/HZSM-5 system, Cu incorporated ZSM-5 is tested for acetone conversion. From Table 7, 100% acetone conversion can be obtained at 83 $g.h.mol^{-1}$, as compared to 67.5% from the physical mixed bed at 76+7 $g.h.mol^{-1}$ (Table 6). It is worth noting that a zeolite with higher Si/Al is used for the bi-functional catalyst in order to keep the number of acid sites and metal loadings the same as in the physical mixed bed system. Despite of that, a remarkable increase in activity, as compared to physical mixed catalyst, is probably due to the close proximity for the metal and the acid site. The hydrogenated intermediate, 2-propanol, may well be removed immediately by dehydration over a near-by acid sites, diminishing reversible dehydrogenation of the 2-propanol formed back to acetone. This successive dehydration of 2-propanol to propylene would significantly increase the rate of acetone conversion over the Cu catalysts. In line with this view, the turnover frequency for hydrodeoxygenation (11.8×10^{-3} sec^{-1}) is approximately four-fold higher than that of hydrogenation (2.6×10^{-3} sec^{-1}) at 473 K (Table S2). However, propane is also produced over the bi-functional catalyst, probably via the hydrogen transfer. It is likely that, at high contact time, propylene can be adsorbed onto the acid site. The hydrogenation of the adsorbed propylene may well be promoted by metal-acid site interaction. In other words, the adsorbed hydrogen on the metal can be source of hydrogen transfer to the adsorbed olefin on the proximate acid site. It should be noted that

direct hydrogenation of propylene over copper metal surface is not the case, as evidenced and discussed previously. The propylene hydrogenation can be diminished by the decrease in contact time. This is because relatively small amount of propylene can be adsorbed on the acid site when large amount of alcohol is present in the reaction stream. For a comparison, 5%Cu/HY (100) shows a higher acetone conversion. This is because the HY (100) possesses a higher adsorption and dehydration activity, as compared to HZSM-5 (250) as discussed earlier

Over 5%Cu/HY (100), the activity is in the order of MEK < cyclohexanone < acetone, respectively. The observed low activity for MEK is due to a rapid deactivation as seen by relatively higher carbon deposit shown in Table 3. As discussed previously, oligomerization is increasingly promoted for the larger ketone, particularly over the catalyst with larger pore opening such as HY. Accordingly, as the catalyst is deactivating, the observed activity of cyclohexanone conversion at 6^{th} hours on stream become slightly lower than that of acetone, despite cyclohexanone shows a higher conversion over the mixed catalyst (Table 6). This is because the large pore size with the cage structure of Y enhances the oligomerization of cyclohexanone, as compared to that over the medium channel of HZSM-5. The amount of coke deposit is in line with the observed activity (Table 3).

4. Conclusion

The optimization of reaction conditions and catalyst system for both hydrogenation and dehydration leads to a potential approach for ketone deoxygenation to olefins. Nickel catalyst is more reactive than the copper, but it is also capable to promote hydrogenation of the olefin produced. Accordingly, a double bed system containing Ni/SiO_2 and zeolites is ideal for ketone hydrodeoxygenation to olefins. In contrast, the mixed Cu/SiO2-zeolites and Cu/zeolites can be used for single bed system. For the latter case, copper can hydrogenate ketone to alcohol without hydrogenolysis and it is somewhat inert for olefin hydrogenation. While zeolite can promote dehydration of the alcohol formed at the same temperature range ($\leq$ 473 K). A close-proximity found in Cu/zeolites synergistically promotes the activity towards olefin formation as the alcohol formed is subsequently removed over the neighboring acid sites. The simultaneous conversion of alcohol to alkene, observed in both single bed systems, boost the ketone conversion to exceed the ketone-alcohol equilibrium level.

Acknowledgement

The authors are grateful for a financial support from the Thailand Research Fund through the Royal Golden Jubilee Ph.D. Program (Grant No. PHD/0137/2553) and assistance from PTT Public Co. Ltd.,.

Note

[a]*Department of Chemistry, Faculty of Science, King Mongkut's Institute of Technology Ladkrabang, Chalongkrung Road, Bangkok 10520, Thailand*

[b]*Catalytic Chemistry Research Unit, Faculty of Science, King Mongkut's Institute of Technology Ladkrabang, Chalongkrung Road, Bangkok 10520,*

E-mail: kstawan@kmitl.ac.th; Fax: +662-326-4415; Tel: +6681-929-8288

376 **References**

1 C. A. Mullen and A. A. Boateng, *Energy Fuels,* 2008, **22**, 2104-2109.

2 M. F. Demirbas, *Energy Sources Part A,* 2010, **32**, 909-916.

3 S. Suttibak, *Proc. Sci. Eng.,* 2013, **2013**, 338-343.

4 D. C. Elliott, T. R. Hart, G. G. Neuenschwander, L. J. Rotness and A. H. Zacher, *Environ. Prog. Sustainable Energy,* 2009, **28**, 441-449.

5 E. G. Baker and D. C. Elliott, *Catalytic Hydrotreating of Biomass-Derived Oils,* first ed., American Chemical Society, 1988.

6 J. Wildschut, I. Melián-Cabrera and H. J. Heeres, *Appl. Catal., B,* 2010, **99**, 298-306.

7 C. A. Fisk, T. Morgan, Y. Ji, M. Crocker, C. Crofcheck and S. A. Lewis, *Appl. Catal., A,* 2009, **358**, 150–156.

8 M. A. Naylor, US patent, **3271447**, 1966.

9 E. Sert and F. S. Atalay, *Ind. Eng. Chem. Res.,* 2012, **51**, 6666-6671.

10 C. T. Kautter and U. Baumann, US patent, **3458561**, 1969.

11 L. Wu, G. Wang and X. Chen, US patent, **6420307B1**, 2002.

12 P. G. Menon, *J. Catal.,* 1979, **50**, 314-316.

13 L. Forni, M. Tescari and P. Zambelli, *J. Catal.,* 1980, **65**, 470-474.

14 Y. Liu, K. Murata, M. Inaba and N. Mimura, *Catal. Lett.,* 2003, **89**, 49-53.

15 S. Ghosh, S. S. Acharyya, R. Tiwari, B. Sarkar, R. K. Singha, C. Pendem, T. Sasaki and R. Bal, *ACS Catal.,* 2014, **4**, 2169−2174.

16 M. O. Robeson and T. P. Webb, US patent, **2623909**, 1952.

17 L. P. Silva and E. F. Barbosa, *Polypropylene*, Nova Science Publishers, Inc., 2013.

18 L. Y. Zhang, G. Q. Fan, C. Y. Guo, J. Y. Dong, Y. L. Hu and M. B. Huang, *Eur. Polym. J.,* 2006, **42**, 1043–1050.

19 P. Sun, M. Heng, S. H. Sun and J. Chen, *Energy Convers. Manage.,* 2011, **52**, 924–933.

20 A. Demirbas, *Energy Convers. Manage.,* 2000, **41**, 633-646.

21 M. A. Serio, E. Kroo and M. A. Wójtowicz, *Prepr. Pap. Am. Chem. Soc., Div. Fuel Chem.,* 2003, **48**, 584-589.

22 K. Ross and G. Mazza, *World J. Agric. Sci.,* 2011, **7**, 763-776.

23 C. Song, A. Pawlowski, J. Ji, S. Shan and Y. Cao, *Environ. Prot. Eng.,* 2014, **40**, 35-43.

24 T. N. Pham, T. Sooknoi, S. P. Crossley and D. E. Resasco, *ACS Catal.,* 2013, **3**, 2456-2473.

25 C. A. Gaertner, J. C. Serrano-Ruiz, D. J. Braden and J. A. Dumesic, *J. Catal.,* 2009, **266**, 71-78.

26 T. N. Pham, D. Shi and D. E. Resasco, *J. Catal.,* 2014, **314**, 149-158.

27 M. Acke and M. Anteunis, *Bull. SOC. Chim. Belges,,* 1965, **74**, 41-51.

28 A. F. Trasarti, N. M. Bertero, C. R. Apesteguía and A. J. Marchi, *Appl. Catal., A,* 2014, **475**, 282–291.

29 G. D. Yadav and R. K. Mewada, *Catal. Today,* 2012, **198**, 330– 337.

30 J. Deng, C. Lu, G. Yang and Z. Chen, *React. Funct. Polym.,* 2012, **72**, 378–382.

31 A. Witsuthammakul and T. Sooknoi, *Appl. Catal., A,* 2012**, 413– 414**, 109– 116.

32 A. Rahman, *Bull. Chem. Reac. Eng. Catal.,* 2010, **5**, 113 – 126.

33 C. T. H. Stoddart and C. Kemball, *J. Colloid Sci.,* 1956, **11**, 532-542.

34 S. Qia, B. A. Cheney, R. Zheng, W. W. Lonergan, W. Yub and J. G. Chen, *Appl. Catal., A,* 2011, **393**, 44–49.

35 T. M. Yurieva, L. M. Plyasova, O. V. Makarova and T. A. Krieger, *J. Mol. Catal. A: Chem.,* 1996, **113**, 455-468.

36 R. Vidruk, M. V. Landau, M. Herskowitz, V. Ezersky and A. Goldbourt, *J. Catal.,* 2011, **282**, 215–227.

37 W. H. Wade, S. Teranishi and J. L. Durham, *J. Colloid Interface Sci.,* 1966, **21**, 349-357.

38 P. A. Jacobs, W. J. Mortier and J. B. Uytterhoeven, *J. Inorg, Nucl. Chem.,* 1987, **40**, 1919-1923.

39 F. S. Stone and A. L. Agudo, *Z Phys. Chem. Neue. Fol.,* 1969, **64**, 161—170.

40 A. Ausavasukhi and T. Sooknoi, *Appl. Catal., A,* 2009, **361**, 93–98.

41 N. Peamaroon and T. Sooknoi, *Pet. Sci. Technol.,* 2012, **30**, 1647–1655.

42 D. L. Hoang, T. T. H. Dang, J. Engeldinger, M. Schneider, J. Radnik, M. Richter and A. Martin, *J. Solid State Chem.,* 2011, **184**, 1915–1923.

43 G. V. Sagar, P. V. R. Rao, C. S. Srikanth and K. V. R. Chary, *J. Phys. Chem. B,* 2006, **110**, 13881-13888.

44 A. Ausavasukhi, S. Suwannaran, J. Limtrakul and T. Sooknoi, *Appl. Catal., A,* 2008, **345**, 89–96.

45 W. S. Chen, F. W. Chang, L. S. Roselin, T. C. Ou and S. C. Lai, *J. Mol. Catal. A: Chem.,* 2010, **318**, 36–43.

46 H. S. Roh, W. S. Dong, K. W. Jun, Z. W. Liu, S. E. Park and Y. S. Oh, *Bull. Korean Chem. Soc.,* 2002, **23**, 669-673.

47 N. Yao, H. Ma, Y. Shao, C. Yuan, D. Li and X. Li, *J. Mater. Chem.,* 2011, **21**, 17403-17412.

48 S. Esposito, S. D. Vecchio, G. Ramis, M. Bevilacqua, M. Turco, G. Bagnasco, C. Cammarano, A. Aronne and P. Pernice, *Chem. Eng. Trans.,* 2007, **11**, 83-88.

49 C. W. Tang, C. B. Wang and S. H. Chien, *Thermochim. Acta,* 2008, **473**, 68–73.

50 N. A. M. Nasir, N. A. M. Zabidi and C. F. Kait, *J. Appl. Sci.,* 2011, **11**, 1391-1395.

51 C. H. Zhang, H. J. Wan, Y. Yang, H. W. Xiang and Y. W. Li, *Catal. Commun.,* 2006, **7**, 733–738.

52 X. Ge, H. Zou, J. Wang and J. Shen, *React. Kinet. Catal. Lett.,* 2005, **85**, 253-260.

53 C. S. Kim and S. I. Woo, *J. Mol. Catal.,* 1992, **73**, 249-263.

54 Z. Strassberger, A. H. Alberts, M. J. Louwerse, S. Tanase and G. Rothenberg, *Green Chem.,* 2013, **15**, 768-774.

55 C. Huo, J. Ouyang and H. Yang, *Sci. Rep.,* 2014, **4**, 1-9.

56 R. S. Mann and T. R. Lien, *J. Catal.,* 1969, **15**, 1-7.

57 L. Brandao, D. Fritsch, L. M. Madeira and A. M. Mendes, *Chem. Eng. J.,* 2004, **103**, 89–97.

58 S. Sitthisa and D. E. Resasco, *Catal. Lett.,* 2011, **141**, 784–791.

59 X. Fang, X. Min, L. X. Feng and H. X. Lan, *J. Therm. Sci.,* 2013, **22**, 613-618.

60 W. Mooksuwan and S. Kumar, *Int. J. Energy Res.,* 2000, **24**, 1109-1122.

61 E. Buckley an E.F.G. Herington, *Trans. Faraday Soc.,* 1965, **61**, 1618-1625.

62 P. Nash, *Phase diagrams of binary nickel alloys*, ASM International, 1991.

63 J. A. Rodriguez and D. W. Goodman, *J. Phys. Chem.,* 1990, **94**, 5342-5347.

64 H. J. Solomon, H. Bliss and J. B. Butt, *Ind. Eng. Chem. Fundamen.,* 1967, **6**, 325–333.

65 M. L. Occelli, J. T. Hsu and L. G. Galya, *J. Mol. Catal.,* 1985, **32**, 377 – 390.

66 T. Tago, H. Konno, S. Ikeda, S. Yamazaki, W. Ninomiya, Y. Nakasaka and T. Masuda, *Catal. Today,* 2011, **164**, 158–162.

67 A. J. Cruz-Cabeza, D. Esquivel, C. Jiménez-Sanchidrián and F. J. Romero-Salguero, *Mater.,* 2012, **5**, 121-134.

Selective Hydrodeoxygenation of Bio-Oil Derived Products: Ketones to Olefins

Ayut Witsuthammakul and Tawan Sooknoi*

Graphical Abstract

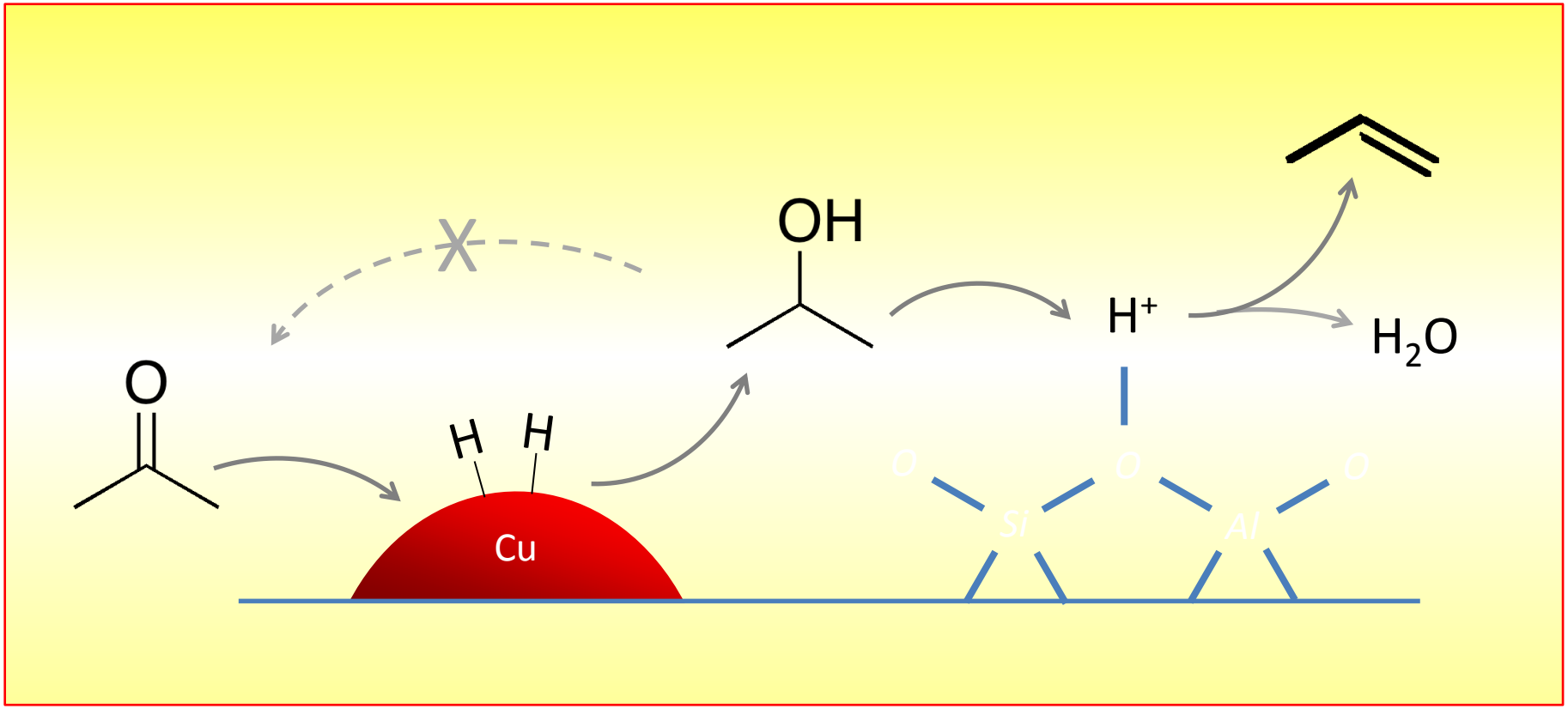

Hydrogenation of a ketone primarily takes place on the metal surface resulting in a corresponding alcohol that can be dehydrated to olefin over the acid function. A rapid dehydration synergistically prevent reversible dehydrogenation of alcohol while excessive olefin hydrogenation can be limited over selected metal.

Selective Hydrodeoxygenation of Bio-Oil Derived Products: Ketones to Olefins

Ayut Witsuthammakul and Tawan Sooknoi*

Table & Figure

Table 1 Copper surface area, copper dispersion, and acidity of Cu catalysts

Catalyst	Cu area (m^2/g_{Cu})	% Cu dispersion	Acidity (μmol/g)	
			Weak	Strong
2%Cu/SiO_2	257	n/a	-	-
5%Cu/SiO_2	646	95	-	-
10%Cu/SiO_2	437	66	-	-
15%Cu/SiO_2	220	24	-	-
5%Cu/HY (100)[a]	499	65	158	62
HY (100) [a]	-	-	54	65
5%Cu/HZSM-5 (250) [a]	414	54	-	-

[a]*Number in the parenthesis represents Si/Al of the sample*

Table 2 Initial activated temperature for hydrogenation and hydrogenolysis over metal catalysts from 373 – 623 K

Catalyst	Initial activated temperature[a]		
	Acetone hydrogenation to i-propanol	Acetone hydrogenolysis to paraffins	Propylene hydrogenation to propane
2%Cr/SiO_2	inactive	inactive	-
10%Cr/SiO_2	inactive	inactive	-
2%Fe/SiO_2	inactive	inactive	-
10%Fe/SiO_2	473K	inactive	523K
2%Co/SiO_2	523K	523K	498K
2%Ni/SiO_2	< 373K	473K	< 398K
2%Cu/SiO_2	< 373K	Inactive	Inactive
2%NiCu/SiO_2 [50:50]	< 373K	573K	< 473K
2%Pd/SiO_2	423K	573K	Active [58-59]

[a]*Temperature at which >3% conversion is obtained over the catalyst at W/F of 30 g.h.mol^{-1}, H_2 as carrier 30 m/min*

Table 3 Thermo-gravimetric analysis of spent catalysts

Catalyst	Feed	Temp	Contact time	Weight loss (%)		
		K	(g.h.mol^{-1})	473-573 K	>573 K	Total
5%Ni/SiO_2	Acetone	448	15	-	-	-
5%Cu/SiO_2	Acetone	473	15	-	-	-
HY(7.5)	Acetone	448	3	-	2.6	2.6
H-β(14)	Acetone	448	3	-	5.5	5.5
H-Mordenite(15)	Acetone	448	15	2.1	5.4	7.5
HZSM-5(13)	Acetone	448	15	6.1	0.88	7.0
HZSM-5 (13); TGA in N_2	Acetone	448	15	5.9	0.00	5.9
5%Cu/SiO_2+HZSM-5(13)	Acetone	473	76+7	1.9	2.2	4.1
	MEK	473	76+7	2.1	2.4	4.5
	Cyclohexanone	473	76+7	2.0	2.0	4.0
5%Cu/SiO_2+H-β(14)	Acetone	473	76+7	1.3	1.9	3.2
	Acetone	473	76+2	1.6	1.0	2.6
5%Cu/HY(100)	Acetone	473	19	1.9	1.3	3.2
	MEK	473	19	4.3	2.1	6.4
	Cyclohexanone	473	19	2.8	1.6	4.4

air-zero, 10K/min

Table 4 Effect of zeolite frameworks to *i*-propanol and di-isopropyl ether dehydration

Zeolite (Si/Al)	**Feed**	**Contact time**	**Conversion**	**Selectivity** (C mol%)			
		(g.h.mol^{-1})	(C mol%)	Propylene	Di-isopropyl ether	*i*-propanol	C6 olefins
HY (8)*	*i*-propanol	3	18.0	51.4	48.6	-	-
H-β (14)	*i*-propanol	3	58.8	90.3	9.69	-	-
HY (8)	*i*-propanol	15	89.5	99.6	0.37	-	-
H-β (14)	*i*-propanol	15	99.5	100	0.00	-	-
H-Mordenite (15)	*i*-propanol	15	27.9	80.0	20.0	-	-
HZSM-5 (13)	*i*-propanol	15	54.6	98.0	1.96	-	-
H-β (14)	Di-isopropyl ether	15	83.5	69.4	0.00	28.7	1.93

Results at 6th hour on stream, 448K, H_2 as carrier 30 m/min

**numbers in parenthesis represent Si/Al*

Table 5 Ketones hydrodeoxygenation on 5%Ni/SiO_2 - HZSM-5 (13) double-bed system

Feed	**Contact time** (g.h/mol) 1st bed + 2nd bed	**Conversion** (C mol%)	**Selectivity** (C mol%)			
			Alcohols	**Ethers**	**n-Alkenes**	**i-Alkenes**
Acetone	76+7	61.9	52.2	0.45	47.4	0.00
	76+29	59.9	15.8	0.00	84.2	0.00
MEK	76+7	61.8	39.4	0.00	51.6	9.00
	76+29	58.7	0.00	0.00	87.1	12.9

Result at 6th hour on stream, 448 K, (1st bed+2nd bed), H_2 as carrier 30 ml/min

Table 6 Ketones hydrodeoxygenation on physical mixed 5%Cu/SiO_2 – zeolites

Feed	Catalyst	Temp. (K)	Contact time (g.h/mol) Metal+Zeolite	Conversion (C mol%)	Selectivity (C mol%)				
					Alcohols	n-Alkenes/ cycloalkenes	i-Alkenes/ methyl cycloalkenes	Acetic acid	Mesityl oxide
Acetone	5%Cu/SiO_2 +HZSM-5 (13)	473	76+7	67.5	3.24	95.6	0.00	0.00	0.00
	5%Cu/SiO_2 +H-β (14)	473	76+7	21.1	0.00	75.1	1.12	2.34	16.6
		473	76+2	40.9	5.57	92.1	0.00	0.00	0.00
MEK	5%Cu/SiO_2 +HZSM-5 (13)	473	76+7	56.2	4.36	82.1	13.6	0.00	0.00
Cyclohexanone	5%Cu/SiO_2 +HZSM-5 (13)	473	76+7	100	0.00	95.8	4.21	0.00	0.00
		473	27+3	45.5	43.0	57.0	0.00	0.00	0.00
		423	76+7	57.6	64.3	35.7	0.00	0.00	0.00

Result at 6th hour on stream, H_2 as carrier 30 ml/min

Table 7 Ketones hydrodeoxygenation on 5%Cu/zeolites

Feed	Catalyst	Contact time (g.h/mol)	Conversion (C mol%)	Selectivity (C mol%)			
				Alcohols	**n-Alkenes / cycloalkene**	***i*-Alkenes / methyl cycloalkenes**	**Alkanes**
Acetone	5%Cu/HZSM-5 (250)	83	100	0.00	68.9	0.00	31.1
	5%Cu/HZSM-5 (250)	19	51.6	15.9	81.1	0.00	2.01
	5%Cu/HY (100)	19	90.5	6.3	88.3	0.00	5.40
MEK	5%Cu/HY (100)	19	24.7	0.00	87.3	12.7	0.00
Cyclohexanone	5%Cu/HY (100)	19	85.4	18.2	81.8	0.00	0.00

Result at 6th hour on stream, H_2 as carrier 30 ml/min, *473 K*,

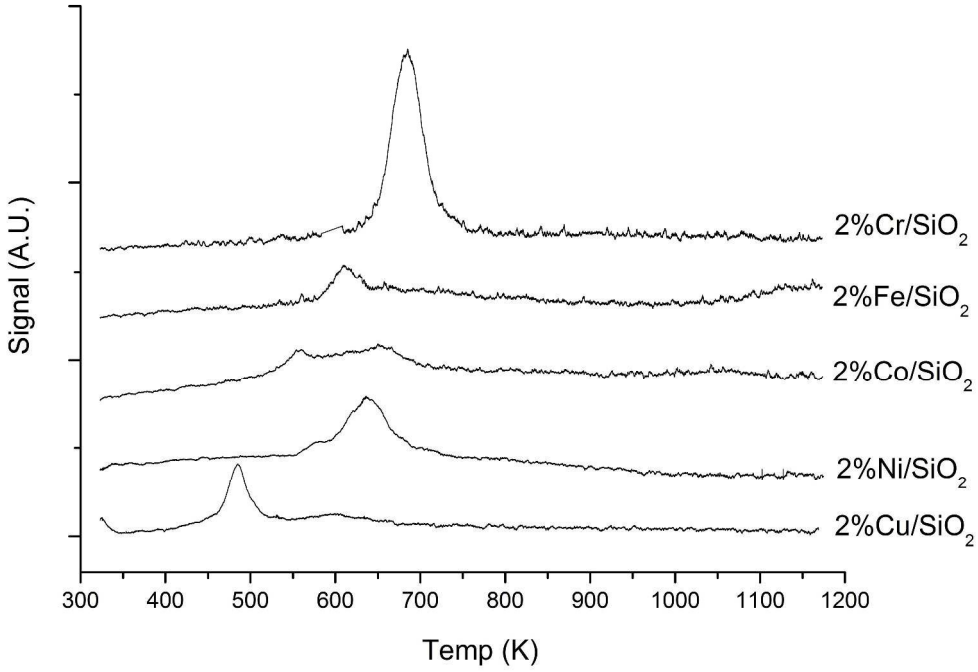

499x353mm (300 x 300 DPI)

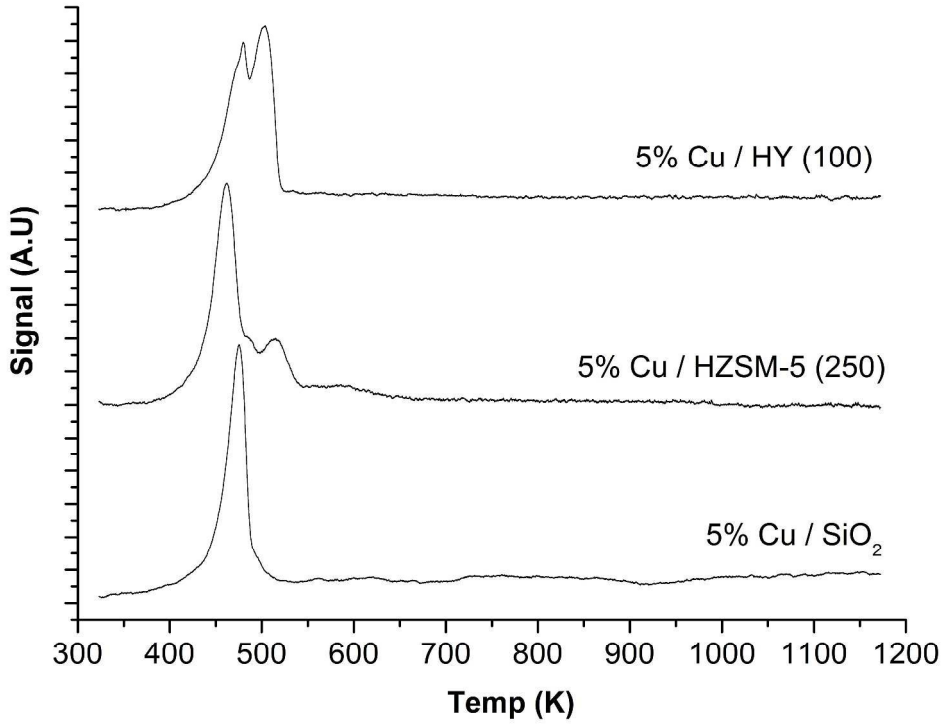

460x353mm (300 x 300 DPI)

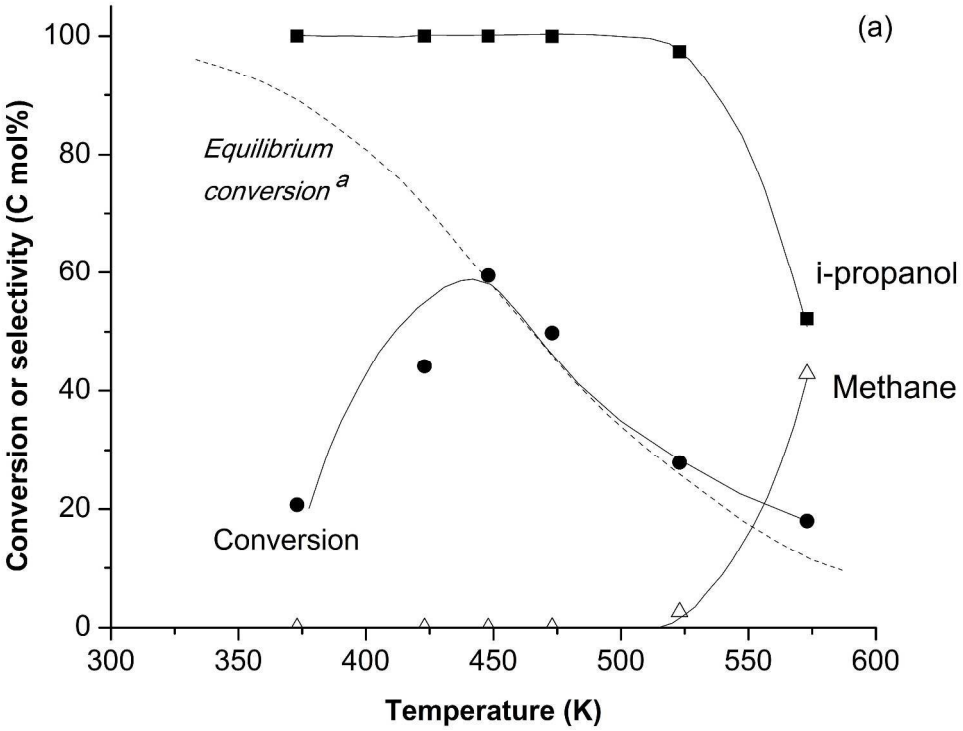

499x378mm (300 x 300 DPI)

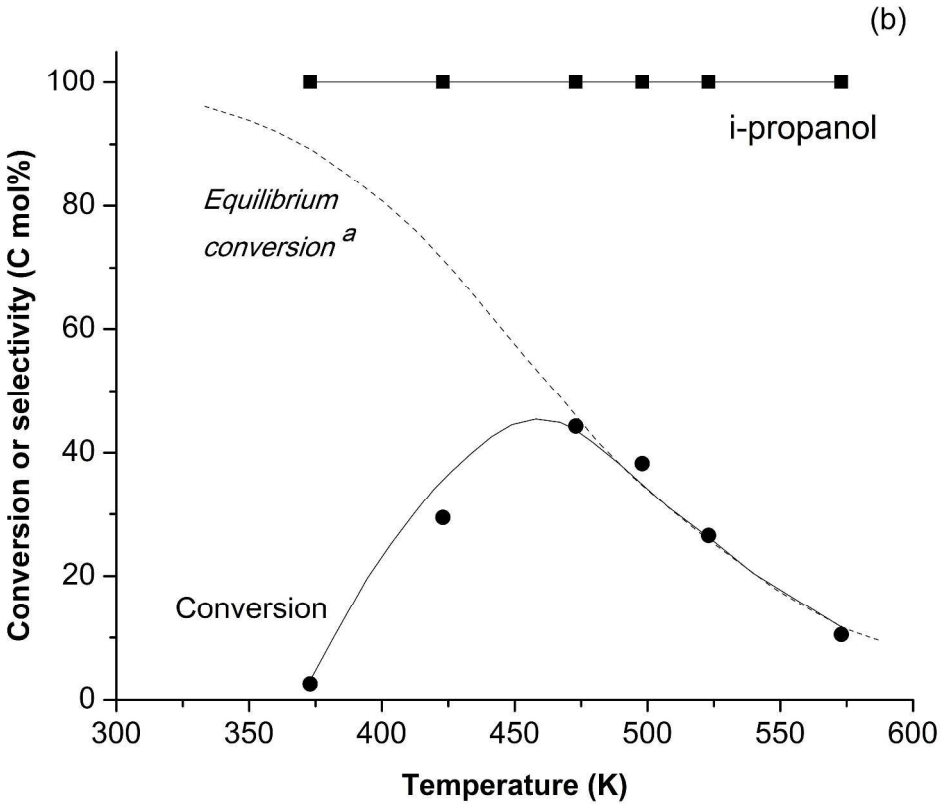

479x405mm (300 x 300 DPI)

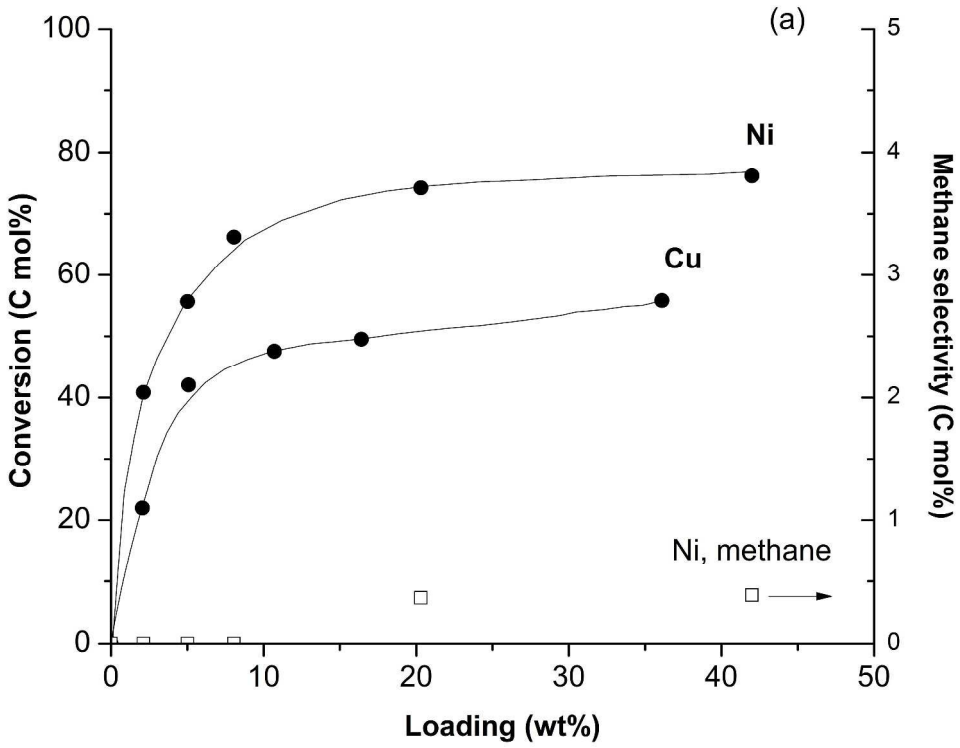

500x396mm (300 x 300 DPI)

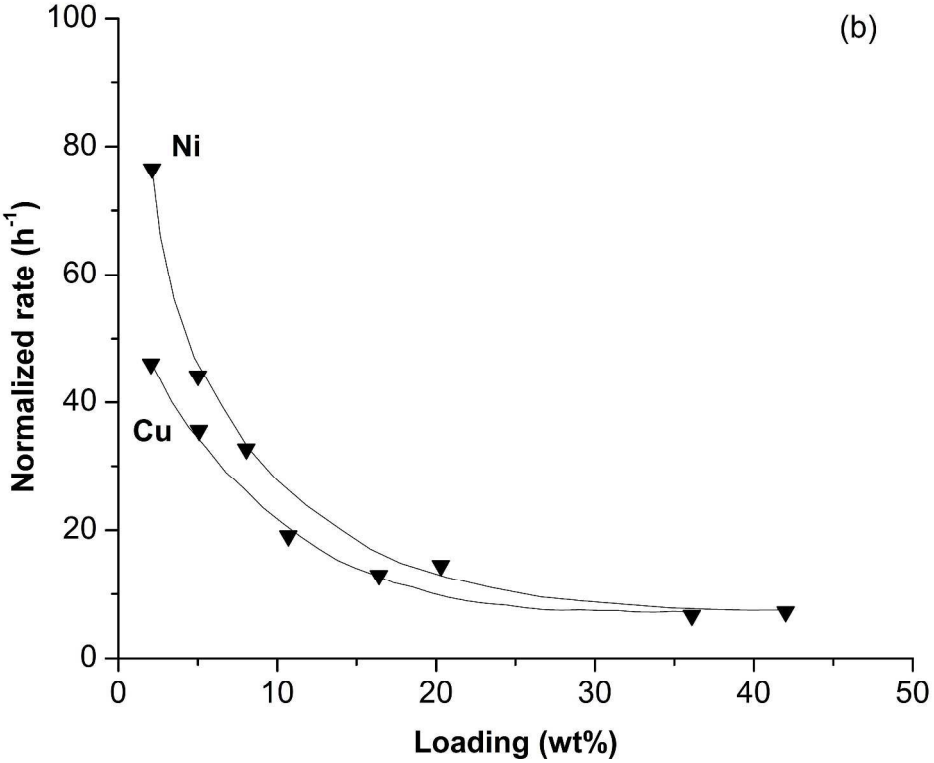

480x389mm (300 x 300 DPI)

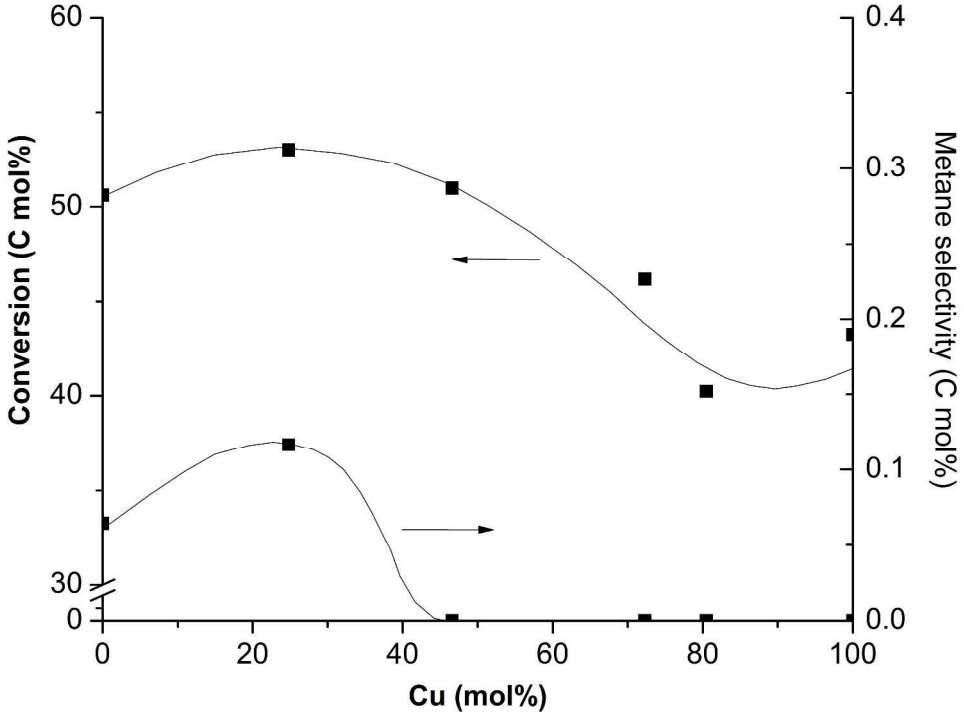

508x386mm (300 x 300 DPI)

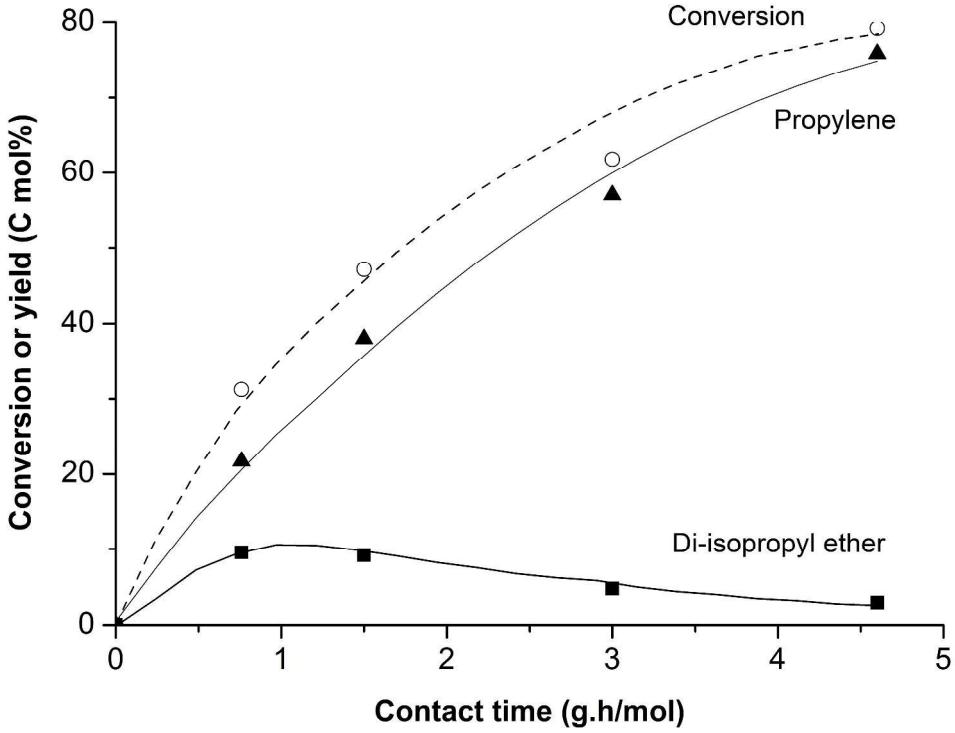

461x351mm (300 x 300 DPI)

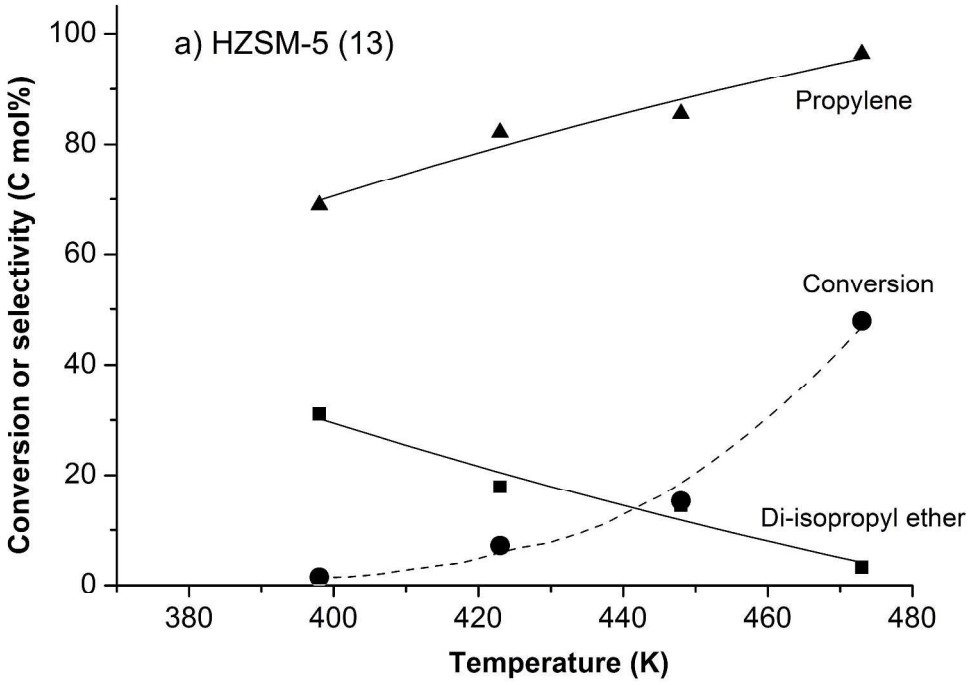

479x346mm (300 x 300 DPI)

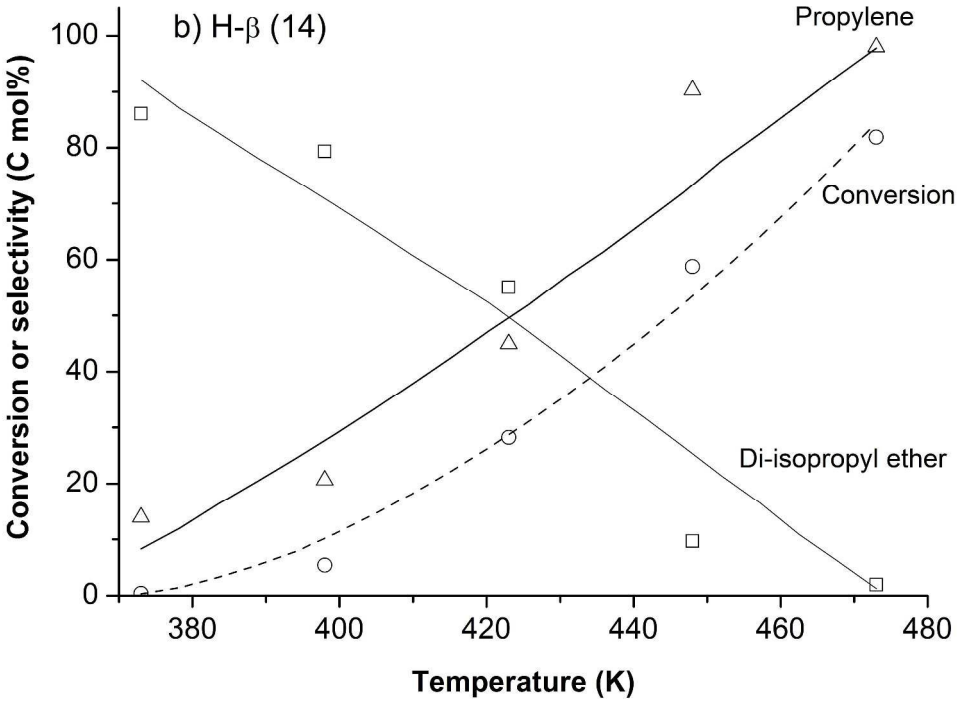

472x346mm (300 x 300 DPI)

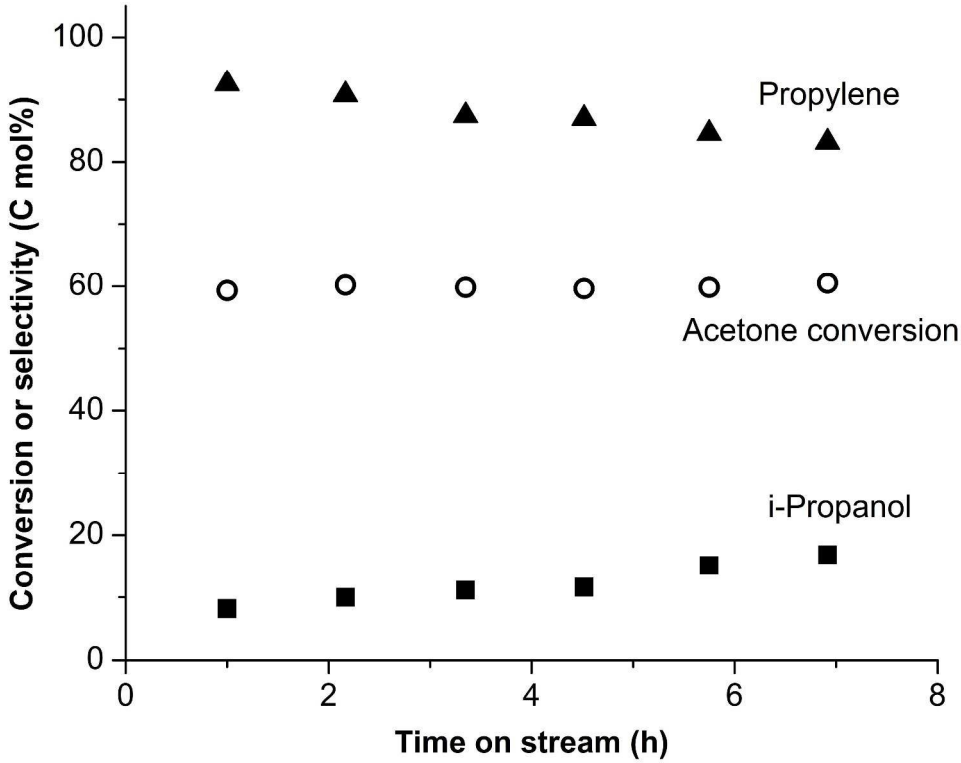

469x377mm (300 x 300 DPI)